European Journal of Radiology 199 (2026) 112766

Contents lists available at ScienceDirect

European Journal of Radiology

journal homepage: www.elsevier.com/locate/ejrad

Assessing coronary in-stent restenosis using ultrahigh-resolution photon-counting detector CT: results from a two-center study

Bálint Szilveszter [a,*], Muhammad Taha Hagar [b], Péter Kulyassa [a], Barbara Sipos [a], Anikó Kubovje [c], Borbála Vattay [a], Melinda Boussoussou [a], Sámuel Beke [c], Kristóf Nagy [c], Lili Száraz [c], Pál Maurovich-Horvat [c], Akos Varga-Szemes [b,c], Tilman Emrich [b,d], Milán Vecsey-Nagy [a,b]

[a] Semmelweis University Heart and Vascular Center, Városmajor Street 68., 1122 Budapest, Hungary
[b] Department of Radiology and Radiological Science, Medical University of South Carolina, 25 Courtenay Dr, Charleston 29425, SC, USA
[c] Department of Radiology, Medical Imaging Centre, Semmelweis University, 2 Korányi Sándor St, 1083 Budapest, Hungary
[d] Department of Diagnostic and Interventional Radiology, University Medical Center of the Johannes Gutenberg-University, Mainz, Germany

ARTICLE INFO

Keywords:
Photon-counting CT detector
Stent assessment
Coronary artery disease
Diagnostic accuracy

ABSTRACT

Introduction: To assess the diagnostic accuracy of ultrahigh-resolution (UHR) photon-counting detector (PCD)-CT for detecting obstructive and non-obstructive coronary in-stent restenosis (ISR), using invasive coronary angiography (ICA) as the reference.

Methods: Consecutive patients with coronary stents who underwent clinically indicated coronary CT angiography (CCTA) on a dual-source PCD-CT were retrospectively identified from two academic centers. All UHR scans were reconstructed at 0.2 mm and 0.4 mm slice thickness, the latter served as an energy-integrating detector CT-like proxy. Series were assessed for the presence of non-obstructive (<50%) and obstructive (≥50%) ISR, with diagnostic accuracy validated against ICA in the overall cohort and in a sub-analysis of stents < 3 mm in diameter.

Results: Fifty patients (16.0% women; 70.9 ± 10.8 years) with 106 coronary stents were included. ICA identified 17 non-obstructive and 27 obstructive ISR. Non-obstructive ISR was detected in 10 stents on 0.2 mm UHR and 14 on 0.4 mm EID-like standard-resolution reconstructions.Obstructive ISR was described in 26 (0.2 mm) vs. 32 (0.4 mm) stents, respectively. The proportion of evaluable stents increased from 91.5% based on 0.4 mm to 99.1% with 0.2 mm UHR. Compared with standard-resolution images, 0.2-mm UHR improved non-obstructive ISR sensitivity (90.5%vs82.9%), specificity (100.0%vs78.5%), and accuracy (96.2%vs80.2%); and in obstructive ISR, specificity (98.7%vs82.3%), positive predictive value (96.3%vs64.1%), and accuracy (98.1%vs84.9%). Thin-slice UHR achieved higher accuracy in small-caliber stents (<3mm), for both non-obstructive (94.1vs73.5%) and obstructive ISR (94.1%vs79.4%).

Conclusion: UHR PCD-CT demonstrated excellent diagnostic accuracy and significant improvements in ISR detection compared to the quasi-standard reconstructions, including non-obstructive and small-caliber stent ISR.

1. Introduction

Persistent or recurrent symptoms after percutaneous coronary intervention (PCI) often indicate complications such as in-stent restenosis (ISR), highlighting the need for reliable non-invasive assessments [1–3]. Coronary CT angiography (CCTA) using energy-integrating detector (EID) technology is increasingly used to assess ISR, but remains limited by suboptimal spatial resolution and metal artifacts. These

Abbreviations: BMS, Bare-Metal Stent; CAD, Coronary Artery Disease; CCTA, Coronary Computed Tomography Angiography; DES, Drug-Eluting Stent; EID-CT, Energy-Integrating Detector Computed Tomography; ICA, Invasive Coronary Angiography; ISR, In-Stent Restenosis; LAD, Left Anterior Descending artery; mSv, Millisievert; PCI, Percutaneous Coronary Intervention; PCD-CT, Photon-Counting Detector Computed Tomography; QIR, Quantum Iterative Reconstruction; SD, Standard Deviation; UHR, Ultrahigh-Resolution.

* Corresponding author.
E-mail address: szilveszter.balint@semmelweis.hu (B. Szilveszter).

https://doi.org/10.1016/j.ejrad.2026.112766
Received 12 January 2026; Received in revised form 3 February 2026; Accepted 3 March 2026
Available online 6 March 2026

limitations have historically impaired lumen assessment, particularly in small stents (<3 mm), with up to 10–15% deemed non-diagnostic [4,5]. Accordingly, recent expert consensus supports the use of CCTA only in symptomatic patients with stents ≥ 3 mm, particularly when proximally located [6,7].

Photon-counting detector (PCD)-CT may overcome the limitations historically associated with EID-CTs, and has been shown to outperform conventional scanners with regard to diagnostic accuracy in coronary assessment [8–10]. This improvement is largely due to the improved spatial resolution of technology, which has been demonstrated to result in significantly improved in-stent lumen delineation in phantom studies [11,12]. The excellent diagnostic performance of PCD-CT has also been demonstrated in vivo; however, prior studies were limited by single-center designs, small stent numbers, lack of comparative reconstructions, and a focus solely on obstructive disease [13].

The current two-center study aimed to evaluate the diagnostic accuracy of ultrahigh-resolution (UHR) PCD-CT for obstructive and non-obstructive ISR across a wide range of stent calibers and compositions, using quantitative coronary angiography (QCA) as the reference standard. Emphasis was placed on comparing 0.2 mm and 0.4 mm slice thickness reconstructions to simulate the incremental value of UHR. By incorporating comparative reconstructions and assessing ISR across non-obstructive and obstructive dimensions, also focusing on stents < 3 mm in diameter, this study sought to address gaps in the literature and support broader clinical adoption of PCD-CT in stent evaluation.

2. Methods

2.1. Patient population

The present HIPAA-compliant study was approved by the institutional review boards (IV/655–3/2022/EKU and 28803–5/2020/EÜIG) and was conducted in accordance with the tenets of the Declaration of Helsinki. Consecutive patients undergoing UHR CCTA between May 2023 and May 2025 were screened retrospectively at two academic centers (Medical University of South Carolina, Charleston, SC, USA; Medical Imaging Centre of Semmelweis University, Budapest, Hungary). Patients over 18 years of age with a documented history of previous coronary stent implantation were included. We excluded patients without invasive coronary angiography (ICA) within 8 weeks of the CCTA. ICA was performed at the treating cardiologist's discretion for clinical indications (suspected ISR by PCD-CT, obstructive CAD in non-stented segments by PCD-CT, or symptom-driven evaluation.

2.2. CT acquisition and reconstruction

CCTA scans were performed on a clinical dual-source PCD-CT system (NAEOTOM Alpha, Siemens Healthineers) in UHR QuantumPlus mode. The gantry rotation time was set at 0.25 s, and the collimation was 120 × 0.2 mm. The tube potential was adjusted to 120/140 kVp, and the image quality level ranged from 50 to 65. Iodinated contrast media was administered within the range of 70 to 100 ml, with a flow rate varying from 4.0 to 5.5 ml/s. All scans were reconstructed using parameters tailored to UHR imaging, including a slice thickness of 0.2 mm, an increment of 0.1 mm, sharp vascular kernels (Bv56–Bv72), and quantum iterative reconstruction (QIR) strength level of 4. Standard-resolution reconstructions were also generated for all patients by downsampling UHR series to 0.4 mm slice thickness with 0.2 mm increment, a softer vascular kernel (Bv40), and QIR level of 4. The clinical acquisition and reconstruction protocols are outlined in Supplementary Table S1.

2.3. CT analysis

CCTA datasets were independently analyzed by two readers with 10 and 8 years of clinical experience in cardiovascular radiology, using commercially available software (syngo.via, version VB60A, Siemens Healthineers). The interpretation of images was conducted using axial, multiplanar, and curved multiplanar reformations, incorporating multiphasic data when necessary. The analysis was conducted exclusively on coronary segments that contained stents. Readers were unaware of the results of the subsequent ICA. Each stent was evaluated visually for the presence and severity of ISR in both standard resolution and UHR reconstructions, which were reviewed in separate sessions in randomized order with a minimum one-week blanking period to mitigate recall bias. The severity of ISR was categorized as follows: negative (0%), non-obstructive (<50%), or obstructive (≥50%), based on a visual assessment [14]. Interpretations were performed both on a per-stent and per-patient basis. Segments that were deemed non-diagnostic were subsequently classified as obstructive, in accordance with an intent-to-diagnose principle. ISR was defined as narrowing occurring within the stent or within 5 mm of the proximal or distal stent edge, consistent with definitions of *peri*-stent restenosis [15]. The inter-observer reproducibility of the findings was subsequently assessed by a cardiovascular radiologist with six years of experience in cardiac CT, who independently reassessed a random subset of 50 stents.

2.4. Quantitative coronary angiography

ICA performed within 8 weeks of CCTA served as the reference standard. All procedures were conducted for clinical indications by board-certified interventional cardiologists using standard techniques. A minimum of five angiographic projections were acquired for the left and right coronary arteries, with at least two orthogonal projections per stented segment. Quantitative coronary angiography (QCA) was performed post-hoc by an interventional cardiologist (P.K.) using dedicated software (Qangio XA 3D 1.1, Medis Medical Imaging System, Leiden, The Netherlands). To facilitate QCA analysis, the location of the stented coronary segment was provided, however, CCTA-based percent diameter stenosis values were fully blinded to the analyst. QCA measurements yielded continuous quantitative values, including reference vessel diameter, minimal luminal diameter, and percentage diameter stenosis. QCA-derived percentage diameter stenosis values were subsequently classified using predefined thresholds as non-obstructive (<50%) or obstructive (≥50%) ISR.

2.5. Statistical analysis

Continuous variables were reported as mean ± standard deviation or median and interquartile range, depending on the distribution. Categorical variables were summarized as counts and percentages. The performance of PCD-CT for the evaluation of ISR was evaluated by calculating sensitivity, specificity, positive predictive value (PPV), negative predictive value (NPV), and overall diagnostic accuracy for the 0.2 mm and 0.4 mm reconstruction datasets. To directly compare diagnostic performance between 0.2 mm and 0.4 mm UHR reconstructions, we applied McNemar's test on paired data for both obstructive and non-obstructive ISR. The ICA reference standard was used for the calculation of these metrics. The evaluation of stents was further stratified by stent caliber, with a cutoff of 3 mm. All diagnostic accuracy metrics were calculated with 95% confidence intervals. The inter-reader agreement for the evaluation of stent patency was assessed using weighted κ on a three-category ordinal ISR scale (none, non-obstructive, obstructive) for 0.2-mm and 0.4-mm reconstructions: ≤ 0.20 indicating no agreement, 0.21–0.40 fair, 0.41–0.60 moderate, 0.61–0.81 substantial, and ≥ 0.82 very strong agreement [16]. A two-sided p-value of less than 0.05 was considered statistically significant. All analyses were performed using IBM SPSS Statistics, version 29.0 (IBM Corp.).

3. Results

3.1. Patient demographics and stent characteristics

A total of 50 patients (16% women; mean age: 70.9 ± 10.8 years) with 106 coronary stents were evaluated. The most common stent location was the left anterior descending artery (LAD) in 39 cases (36.8%), followed by the right coronary artery (RCA) in 36 cases (34.0%), the left circumflex artery (LCX) in 26 cases (24.5%), and the left main (LM) in 1 case (0.9%). Four stents (3.8%) were placed in bypass grafts. The mean stent diameter was 3.14 ± 0.55 mm, among those 34 stents (32.1%) with a diameter below 3 mm. The mean stent length was 23.06 ± 9.59 mm, with longer stents (≥15 mm) in 88 cases (83.0%). Regarding stent composition, cobalt-chromium-based drug-eluting stents (DES) were the most frequently used, accounting for 55 cases (51.9%). Platinum-chromium-based DES were used in 34 cases (32.1%), and bare-metal stents (BMS) composed of stainless steel were present in 17 cases (16.0%). Patient demographics and stent characteristics are summarized in Table 1.

3.2. Diagnostic accuracy of PCD-CT

The mean QCA-derived diameter stenosis was 26.6% ± 36.8%. Non-obstructive ISR was detected in 14 (13.2%), 10 (9.4%), and 17 (16.0%) of the stents using 0.4 mm, 0.2 mm, and ICA, respectively. Obstructive ISR was found in 26 (24.5%) using 0.2 mm, in 32 (30.2%) using 0.4 mm, and in 27 (25.5%) using ICA. Stents were evaluable in 99.1% of all cases based on the 0.2 mm reconstruction versus 91.5% using 0.4 mm reconstruction.

The 0.2 mm UHR reconstruction showed higher sensitivity (90.5%) and specificity (100%) compared to 0.4 mm (sensitivity 82.9%, specificity 78.5%) and a higher diagnostic accuracy (96.2% vs 80.2%), when analyzing stent-based diagnostic performance for detecting less than 50% ISR (Figs. 1 and 2).

When assessing obstructive ISR (≥50%), sensitivity remained high in both standard and UHR reconstructions (96.3% vs 92.6%), but UHR had notably better specificity (98.7% vs 82.3%) and PPV (96.3% vs 64.1%). Diagnostic accuracy was superior with UHR (98.1%) compared to standard resolution (84.9%). Using ICA as the reference standard, patient-based metrics demonstrated similar improvement in diagnostic performance for using the 0.2 mm UHR reconstruction as compared with 0.4 mm standard images. Diagnostic accuracy was substantially higher with UHR versus standard for both non-obstructive and obstructive ISR (Table 2). Inter-reader agreement was higher with 0.2-mm UHR [κ: 0.71 (0.45–0.86)] than with 0.4-mm reconstructions [κ: 0.40 (0.15–0.61)].

Table 1
Patient demographics, CT image acquisition parameters and coronary stent characteristics.

Demographics	N = 50
Age (years)	70.9 ± 10.8
Sex (female, n (%))	8 (16)
BMI (kg/m^2)	28.6 ± 4.6
Cardiovascular risk factors	
Hypertension, n (%)	47 (94)
Hyperlipidemia, n (%)	38 (76)
Diabetes mellitus, n (%)	22 (44)
Smoking history, n (%)	27 (54)
Positive family history, n (%)	21 (42)
CCTA protocol	
Mean effective dose, mSv	8.6 ± 5.1
Mean contrast dose, ml	78.1 ± 5.8
Spiral acquisition, n (%)	37 (74)
Mean heart rate, n (%)	63.6 ± 11.1
Stent location, n (%)	
LM	1 (0.9)
LAD	39 (36.8)
LCX	26 (24.5)
RCA	36 (34.0)
Bypass grafts	4 (3.8)
Stent diameter, mm	3.14 ± 0.55
<3.0, n (%)	34 (32.1)
≥3.0, n (%)	72 (67.9)
Stent length, mm	23.06 ± 9.59
<15 mm, n (%)	18 (17.0)
≥15 mm, n (%)	88 (83.0)
Stent material, n (%)	
Platinum chromium alloy	34 (32.1)
Cobalt chromium alloy	55 (51.9)
BMS- Stainless steel	17 (16.0)

Abbreviations: BMI = Body Mass Index; CCTA = Coronary Computed Tomography Angiography; LM = Left Main; LAD = Left Anterior Descending; LCX = Left Circumflex; RCA = Right Coronary Artery; BMS = Bare-Metal Stent; mSv = Millisievert.

3.3. Accuracy of UHR PCD-CT in small-caliber stents

In our sub-analysis among small-caliber stents (<3 mm), UHR PCD-CT demonstrated superior overall diagnostic accuracy compared to the 0.4 mm mode for both non-obstructive and obstructive ISR detection (Table 3). For non-obstructive lesions, 0.2 mm showed higher specificity (100.0% vs. 66.7%) and PPV (100.0% vs. 61.1%), along with improved overall accuracy (94.1% vs. 73.5%). Similarly, for obstructive lesions, 0.2 mm offered higher specificity (95.8% vs. 75.0%) and accuracy (94.1% vs. 79.4%), supporting its enhanced diagnostic performance in this challenging subgroup.

4. Discussion

Our study demonstrates the excellent diagnostic performance of UHR PCD-CT in detecting ISR in chronic coronary syndrome patients referred for CCTA. High accuracy was observed not only in obstructive lesions but also in non-obstructive cases, making it a more reliable tool for precise stent evaluation. Notably, even small-caliber stents below 3 mm in diameter could be reliably assessed using this technique, which traditionally posed challenges for conventional EID-CT systems.

The use of novel PCD-CT technology provides superior diagnostic accuracy for detecting obstructive lesions in native coronary arteries [8,17]. The optimal combination of kernel, slice thickness, and QIR levels for stent evaluation were reported previously based on combined quantitative and qualitative assessment [18]. Furthermore, Hagar et al. evaluated the role of UHR PCD-CT for the assessment of stent patency in a prospective, single-center study among patients referred for transcatheter aortic valve implantation (TAVI) planning [13]. UHR PCD-CT demonstrated excellent diagnostic performance for detecting obstructive in-stent restenosis, with a per-stent accuracy of 93.2%. Image quality was non-diagnostic in only 3 out of 44 stents for both readers, and in one additional stent for reader 2. ICA confirmed five cases of in-stent restenosis, corresponding to a prevalence of 11.4%. These findings align with comparative in vitro studies showing improved delineation of the in-stent lumen, reduced artifacts using PCD-CT [19]. Our work goes beyond previous investigations by quantifying the magnitude of diagnostic improvements when moving from a thicker slab reconstruction simulating close to EID-CT settings to the 0.2 mm UHR protocol using QCA as reference. Unlike several earlier studies that artificially increased diagnostic accuracy by excluding non-diagnostic stents, our analysis included all stents assessed, reflecting true clinical routine practice, and improves the generalizability of results [20]. Also, the

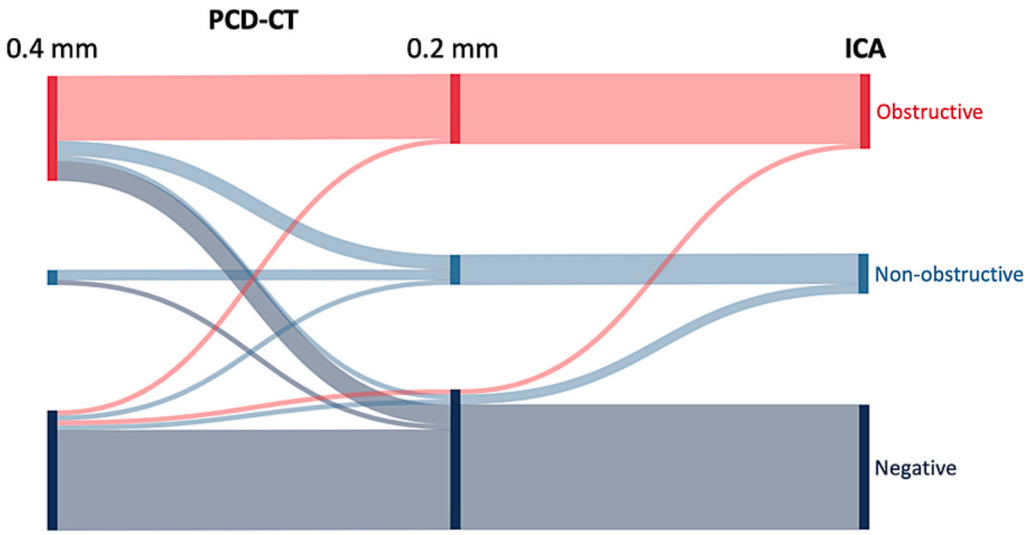

Fig. 1. Sankey diagrams demonstrate reclassification flow of detected in-stent restenosis severity between standard- (0.4 mm), ultrahigh-resolution (0.2 mm) PCD-CT, and ICA. Node and flow widths are proportionate to the number of patients in each diagnostic category. Flow colors reflect the final ICA classification (red = obstructive, blue = non-obstructive, dark navy = negative), allowing visual tracking of individual reclassification pathways and alignment with reference-standard findings. A considerable proportion of obstructive/non-diagnostic findings on 0.4 mm reconstructions were reclassified as non-obstructive or negative on 0.2 mm UHR images, resulting in improved concordance with the invasive reference standard. ICA: Invasive Coronary Angiography; PCD-CT: Photon-counting Detector CT; UHR: Ultrahigh-resolution.

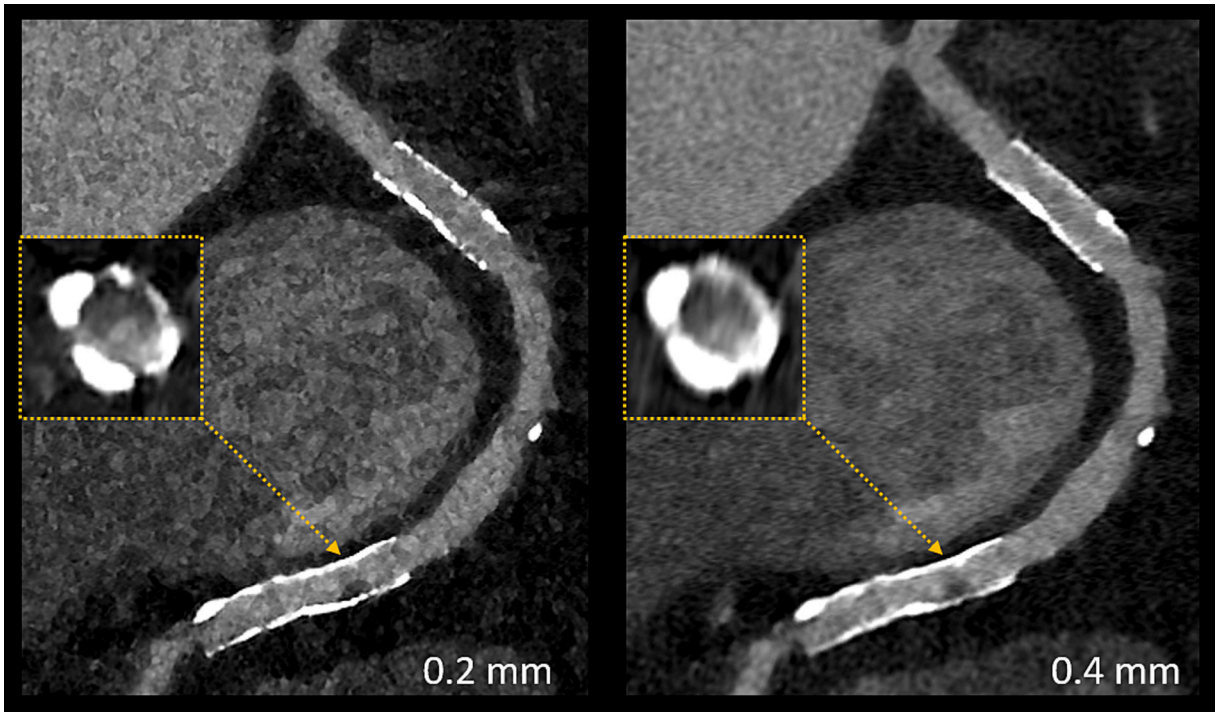

Fig. 2. Ultrahigh-resolution photon-counting detector CT for identifying in-stent restenosis. Comparison of 0.2 mm and 0.4 mm reconstructions in a stented coronary segment of the RCA. The UHR (0.2 mm, Bv64) image demonstrates markedly reduced blooming artifacts and sharp delineation of the stent lumen, leading to classification as non-obstructive ISR. In contrast, the 0.4 mm reconstruction overestimates the luminal narrowing, resulting in an obstructive classification. Invasive coronary angiography confirmed the non-obstructive nature of the lesion. Abbreviations: ISR: In-stent Restenosis; PCD-CT: Photon-counting Detector Computed Tomography; UHR: Ultrahigh-resolution.

current study represents the highest number of coronary stents evaluated to date in the literature. Our stent-based assessment demonstrated excellent diagnostic performance for both non-obstructive and obstructive ISR (Fig. 3). The 0.2 mm reconstruction consistently outperformed the 0.4 mm EID-CT like setting, yielding higher sensitivity, specificity, and accuracy across both ISR categories. Diagnostic accuracy for detecting obstructive ISR reached 98% using the 0.2 mm reconstruction, confirming the added value of high-resolution imaging for challenging stent evaluation. Notably, only one stent was considered non-diagnostic by 0.2 mm UHR PCD-CT, representing a significant improvement compared to the reconstructions mimicking EID-CT settings. Furthermore, as currently demonstrated, accurate detection of

Table 2
Pooled diagnostic accuracy metrics for all stents of 0.2 vs 0.4 mm UHR PCD-CT as compared with ICA as reference.

	0.2 mm UHR	0.4 mm Standard
Stent-based (N = 106)		
Non-obstructive		
Sensitivity, %	90.5 (77.9 – 96.2)	82.9 (68.7 – 91.5)
Specificity, %	100.0 (94.3 – 100.0)	78.5 (67.0 – 86.7)
Positive Predictive Value, %	100.0 (90.8 – 100.0)	70.8 (56.8 – 81.8)
Negative Predictive Value, %	94.1 (85.8 – 97.7)	87.9 (77.1 – 94.0)
Accuracy, %	96.2 (90.7 – 98.5)	80.2 (71.6 – 86.7)
Obstructive		
Sensitivity, %	96.3 (81.7 – 99.3)	92.6 (76.6 – 97.9)
Specificity, %	98.7 (93.2 – 99.8)	82.3 (72.4 – 89.1)
Positive Predictive Value, %	96.3 (81.7 – 99.3)	64.1 (48.4 – 77.3)
Negative Predictive Value, %	98.7 (93.2 – 99.8)	97.0 (89.8 – 99.2)
Accuracy, %	98.1 (93.4 – 99.5)	84.9 (76.9 – 90.5)
Patient-based (N = 50)		
Non-obstructive		
Sensitivity, %	87.0 (67.9 – 95.5)	81.8 (61.5 – 92.7)
Specificity, %	100.0 (86.7 – 100.0)	76.9 (57.9 – 89.0)
Positive Predictive Value, %	100.0 (83.9 – 100.0)	75.0 (55.1 – 88.0)
Negative Predictive Value, %	89.3 (72.8 – 96.3)	83.3 (64.1 – 93.3)
Accuracy, %	93.8 (83.2 – 97.9)	79.2 (65.7 – 88.3)
Obstructive		
Sensitivity, %	93.3 (70.2 – 98.9)	86.7 (62.1 – 96.3)
Specificity, %	100.0 (89.6 – 100.0)	75.8 (59.0 – 87.2)
Positive Predictive Value, %	100.0 (78.5 – 100.0)	61.9 (40.9 – 79.2)
Negative Predictive Value, %	97.1 (85.1 – 99.5)	92.6 (76.6 – 97.9)
Accuracy, %	97.9 (89.1 – 99.6)	79.2 (65.7 – 88.3)

The 95% confidence interval ranges are shown in parentheses. The McNemar's test showed that 0.2 mm reconstructions outperformed 0.4 mm for both obstructive ISR ($p < 0.001$) and non-obstructive ISR ($p < 0.001$), indicating significantly higher accuracy with 0.2 mm reconstructions.
Abbreviations: ICA: Invasive Coronary Angiography; PCD-CT: Photon-counting Detector Computed Tomography; UHR: Ultrahigh-resolution

Table 3
Diagnostic performance in small-caliber stents (<3 mm) using UHR mode with PCD-CT as compared with ICA as reference.

	0.2 mm UHR	0.4 mm Standard
Stent-based (N = 34)		
Non-obstructive		
Sensitivity, %	85.7 (60.1 – 96.0)	84.6 (57.8 – 95.7)
Specificity, %	100.0 (83.9 – 100.0)	66.7 (45.4 – 82.8)
Positive Predictive Value, %	100.0 (75.8 – 100.0)	61.1 (38.6 – 79.7)
Negative Predictive Value, %	90.9 (72.2 – 97.5)	87.5 (64.0 – 96.5)
Accuracy, %	94.1 (80.9 – 98.4)	73.5 (56.9 – 85.4)
Obstructive		
Sensitivity, %	90.0 (59.6 – 98.2)	90.0 (59.6 – 98.2)
Specificity, %	95.8 (79.8 – 99.3)	75.0 (55.1 – 88.0)
Positive Predictive Value, %	90.0 (59.6 – 98.2)	60.0 (35.7 – 80.2)
Negative Predictive Value, %	95.8 (79.8 – 99.3)	94.7 (75.4 – 99.1)
Accuracy, %	94.1 (80.9 – 98.4)	79.4 (63.2 – 89.7)
Patient-based		
Non-obstructive		
Sensitivity, %	71.4 (35.9 – 91.8)	83.3 (43.6 – 97.0)
Specificity, %	100.0 (61.0 – 100.0)	57.1 (25.0 – 84.2)
Positive Predictive Value, %	100.0 (56.6 – 100.0)	62.5 (30.6 – 86.3)
Negative Predictive Value, %	75.0 (40.9 – 92.9)	80.0 (37.6 – 96.4)
Accuracy, %	84.6 (57.8 – 95.7)	69.2 (42.4 – 87.3)
Obstructive		
Sensitivity, %	80.0 (37.6 – 96.4)	80.0 (37.6 – 96.4)
Specificity, %	100.0 (67.5 – 100.0)	62.5 (30.6 – 86.3)
Positive Predictive Value, %	100.0 (51.0 – 100.0)	57.1 (25.0 – 84.2)
Negative Predictive Value, %	88.9 (56.5 – 98.0)	83.3 (43.6 – 97.0)
Accuracy, %	92.3 (66.7 – 98.6)	69.2 (42.4 – 87.3)

The 95% confidence interval ranges are shown in parentheses. Significantly higher accuracy was achieved using 0.2 mm UHR images versus 0.4 mm standard resolution (McNemar's test $p < 0.001$ for both obstructive and non-obstructive comparisons).
Abbreviations: ICA: Invasive Coronary Angiography; PCD-CT: Photon-counting Detector Computed Tomography; UHR: Ultrahigh-resolution

early non-obstructive ISR with PCD-CT is feasible, potentially enabling timely risk stratification and tailored medical management, mitigating progression to clinically significant restenosis, and reducing the need for invasive procedures. Clinically, the use of PCD-CT could improve confidence in excluding or confirming in stent restenosis on noninvasive imaging in symptomatic post-PCI patients. This may help reduce unnecessary referral to invasive coronary angiography when stents are clearly patent, while prioritizing invasive testing for patients with non-evaluable stents or suspected obstructive restenosis.

Current clinical guidelines and appropriate use criteria commonly use a 3 mm stent diameter threshold to recommend or discourage the use of CT for coronary stent evaluation [7,21]. We have shown excellent diagnostic accuracy for detecting both non-obstructive and obstructive ISR even in stents smaller than 3 mm in diameter, signaling an improved visualization capabilities offered by UHR PCD-CT. Future guideline updates will likely reflect this progress, expanding the indications of CCTA. Our bi-centric study design is unique, adding valuable generalizability and robustness to the findings, and reflects more real-world variability in patient populations. In our cohort, 34 stents (32.1%) had a diameter below 3 mm, representing a significant subset of small-caliber stents. The study cohort included stents composed of different materials, including cobalt-chromium-based DES, platinum-chromium-based DES, and stainless-steel BMS to cover commonly used stent options.

We acknowledge the limitations of our study. Importantly, recent updates on the first commercially available PCD-CT scanner allow for combined spectral and UHR image acquisition that can further improve diagnostic performance for certain clinical tasks. Additionally, we employed a reconstruction simulating EID-CT rather than performing a repeat scan in the same patients, avoiding the need for additional radiation exposure in this diagnostic accuracy study. Importantly, we did not use intravascular imaging modalities such as optical coherence tomography or intravascular ultrasound as the reference standard. Our cohort included patients who underwent ICA within 8 weeks after CT, and referral to ICA was at the clinicians' discretion. Because verification by ICA was not applied uniformly and was more likely when PCD-CT suggested disease, partial verification bias may have influenced diagnostic performance. Therefore, further prospective studies are warranted in patients after PCI. Reproducibility metrics showed moderate-to-substantial agreement for ordinal stent assessment. Although this ordinal approach reflects routine clinical decision making, it underscores the importance of optimizing image quality, including the use of sharp reconstruction kernels, 0.2-mm UHR reconstructions, and iterative reconstruction. Recent studies have reported similar reproducibility for classifying obstructive (>50%) ISR (κ = 0.70–0.72) [13,22].

5. Conclusion

This two-center study demonstrated the excellent diagnostic accuracy of UHR PCD-CT for both obstructive and non-obstructive ISR, outperforming 0.4 mm reconstructions, which served as an EID-CT

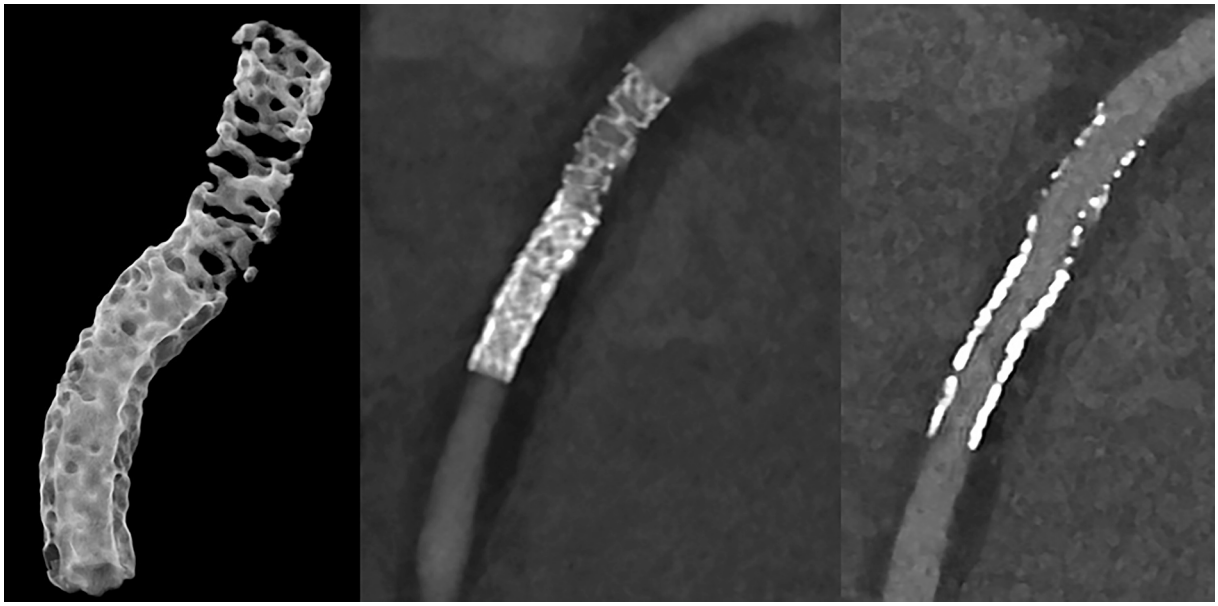

Fig. 3. Representative case of overlapping coronary stent segments assessed with ultrahigh-resolution photon-counting CT. Representative case of a 52-year-old male with effort angina who underwent UHR PCD-CT (Bv56) for the exclusion of ISR following RCA PCI (3.5 mm) and re-PCI using DES (3.5 mm) due to in-stent restenosis. Ultrahigh-resolution PCD-CT ruled out relevant ISR despite overlapping stent segments and provided clear visualization of the stent structure. Abbreviations: PCD-CT: Photon-counting Detector Computed Tomography; PCI: Percutaneous Coronary Intervention; RCA: Right Coronary Artery; UHR: Ultrahigh-resolution.

surrogate. Performance remained high in small-caliber stents, with near-complete evaluability and strong interobserver agreement. These findings support the broader clinical utility of PCD-CT in ISR assessment and provide a rationale for larger prospective studies to confirm clinical impact.

CRediT authorship contribution statement

Bálint Szilveszter: Writing – original draft, Methodology, Formal analysis, Data curation, Conceptualization. **Muhammad Taha Hagar:** Investigation, Data curation. **Péter Kulyassa:** Investigation. **Barbara Sipos:** Investigation. **Anikó Kubovje:** Investigation, Data curation. **Borbála Vattay:** Writing – review & editing, Methodology. **Melinda Boussoussou:** Investigation. **Sámuel Beke:** Visualization. **Kristóf Nagy:** Visualization. **Lili Száraz:** Methodology, Investigation. **Pál Maurovich-Horvat:** Writing – review & editing, Supervision, Resources. **Akos Varga-Szemes:** Writing – review & editing, Supervision, Resources. **Tilman Emrich:** Writing – review & editing, Supervision, Resources. **Milán Vecsey-Nagy:** Writing – review & editing, Software, Methodology, Formal analysis, Conceptualization.

Funding

Bálint Szilveszter was supported by the János Bolyai Research Scholarship of the Hungarian Academy of Sciences. This author was supported by the STARTING 150493 of the Hungarian National Research Development and Innovation Office. Project no. RRF-2.3.1-21-2022-00003 has been implemented with the support provided by the European Union. Borbála Vattay was supported by the EKÖP-2024-180, Semmelweis University Excellence Scholarship Program. Melinda Boussoussou was supported by the EKÖP-2024-187, Semmelweis University Excellence Scholarship Program. Lili Száraz was supported by the Ministry of Culture and Innovation of Hungary from the National Research, Development and Innovation Fund, financed under the KDP-2023 funding scheme, Project No. 2023-2.1.2-KDP-2023-00016.

Declaration of competing interest

The authors declare the following financial interests/personal relationships which may be considered as potential competing interests: [Bálint Szilveszter receives speaker fee and travel support from Siemens Healthineers. Pál Maurovich-Horvat receives speaker fee, travel support, and institutional research support from Siemens. Akos Varga-Szemes receives research support from Siemens and Bayer Healthcare and is a consultant / shareholder at Elucid Bioimaging. Tilman Emrich receives speaker fee, travel support, and institutional research support from Siemens and is a consultant for Circle Cardiovascular Imaging. Milán Vecsey-Nagy is a consultant for Elucid Bioimaging and receives travel support and speaker fees from Siemens Healthineers.

Siemens Healthineers provided technical support for protocol setup and system operation for PCD-CT. Siemens Healthineers had no role in study design, data collection, image interpretation, statistical analysis, or manuscript drafting, and had no influence on the results, their interpretation, or the decision to publish.].

Appendix A. Supplementary data

Supplementary data to this article can be found online at https://doi.org/10.1016/j.ejrad.2026.112766.

References

[1] F. Alfonso, A. Kastrati, Clinical burden and implications of coronary interventions for in-stent restenosis, EuroIntervention 17 (2021) e355–e357.
[2] D. Andreini, S. Mushtaq, D. Trabattoni, et al., Diagnostic accuracy of dynamic stress myocardial CT perfusion compared with invasive physiology in patients with stents: the advantage 2 study, Radiology 313 (2024) e232225.
[3] D. Andreini, G. Pontone, S. Mushtaq, et al., Diagnostic accuracy of coronary CT angiography performed in 100 consecutive patients with coronary stents using a whole-organ high-definition CT scanner, Int. J. Cardiol. 274 (2019) 382–387.
[4] T. Dai, J.R. Wang, P.F. Hu, Diagnostic performance of computed tomography angiography in the detection of coronary artery in-stent restenosis: evidence from an updated meta-analysis, Eur. Radiol. 28 (2018) 1373–1382.
[5] J. Eckert, P. Renczes-Janetzko, M. Schmidt, A. Magedanz, T. Voigtlander, A. Schmermund, Coronary CT angiography (CCTA) using third-generation dual-source CT for ruling out in-stent restenosis, Clin. Res. Cardiol. 108 (2019) 402–410.
[6] G. Pontone, A. Rossi, M. Guglielmo, et al., Clinical applications of cardiac computed tomography: a consensus paper of the European association of

cardiovascular imaging-part I, Eur. Heart J. Cardiovasc. Imaging 23 (2022) 299–314.
[7] J. Narula, Y. Chandrashekhar, A. Ahmadi, et al., SCCT 2021 expert consensus document on coronary computed tomographic angiography: a report of the society of cardiovascular computed tomography, J. Cardiovasc. Comput. Tomogr. 15 (2021) 192–217.
[8] M. Vecsey-Nagy, G. Tremamunno, U.J. Schoepf, et al., Coronary plaque quantification with ultrahigh-spatial-resolution photon-counting detector CT: intraindividual comparison with energy-integrating detector CT, Radiology 314 (2025) e241479.
[9] M. Vecsey-Nagy, G. Tremamunno, U.J. Schoepf, et al., Intraindividual comparison of ultrahigh-spatial-resolution photon-counting detector CT and energy-integrating detector CT for coronary stenosis measurement, Circ. Cardiovasc. Imaging 17 (2024) e017112.
[10] D. Kravchenko, M.T. Hagar, M. Vecsey-Nagy, et al., Value of ultrahigh-resolution photon-counting detector computed tomography in cardiac imaging, Echocardiography 42 (2025) e70100.
[11] E.K. Koons, J.E. Thorne, N.R. Huber, et al., Quantifying lumen diameter in coronary artery stents with high-resolution photon counting detector CT and convolutional neural network denoising, Med. Phys. 50 (2023) 4173–4181.
[12] T. Stein, M.C. von Zur, N. Verloh, et al., Evaluating small coronary stents with dual-source photon-counting computed tomography: effect of different scan modes on image quality and performance in a phantom, Diagn. Interv. Radiol. 31 (2025) 29–38.
[13] M.T. Hagar, M. Soschynski, R. Saffar, et al., Ultra-high-resolution photon-counting detector CT in evaluating coronary stent patency: a comparison to invasive coronary angiography, Eur. Radiol. 34 (2024) 4273–4283.
[14] T. Gaspar, D.A. Halon, B.S. Lewis, et al., Diagnosis of coronary in-stent restenosis with multidetector row spiral computed tomography, J. Am. Coll. Cardiol. 46 (2005) 1573–1579.
[15] D. Andreini, G. Pontone, S. Mushtaq, et al., Coronary in-stent restenosis: assessment with CT coronary angiography, Radiology 265 (2012) 410–417.
[16] M.L. McHugh, Interrater reliability: the kappa statistic, Biochem Med (zagreb) 22 (2012) 276–282.
[17] B. Vattay, B. Szilveszter, M. Boussoussou, et al., Impact of virtual monoenergetic levels on coronary plaque volume components using photon-counting computed tomography, Eur. Radiol. 33 (2023) 8528–8539.
[18] B. Vattay, M. Boussoussou, M. Vecsey-Nagy, et al., Qualitative and quantitative image quality of coronary CT angiography using photon-counting computed tomography: standard and Ultra-high resolution protocols, Eur. J. Radiol. 175 (2024) 111426.
[19] A.E. Michael, D. Schoenbeck, J. Becker-Assmann, et al., Coronary stent imaging in photon counting computed tomography: optimization of reconstruction kernels in a phantom, Eur. J. Radiol. 166 (2023) 110983.
[20] F. Cademartiri, J.D. Schuijf, F. Pugliese, et al., Usefulness of 64-slice multislice computed tomography coronary angiography to assess in-stent restenosis, J. Am. Coll. Cardiol. 49 (2007) 2204–2210.
[21] F. Erthal, M. Premaratne, Y. Yam, et al., Appropriate use criteria for cardiac computed tomography: does computed tomography have incremental value in all appropriate use criteria categories? J. Thorac. Imaging 33 (2018) 132–137.
[22] Y. Gao, Y. Yang, Q. Hu, et al., Photon counting CT improves coronary stent imaging and fat attenuation index assessment across reconstruction modes, Eur J Radiol Open 15 (2025) 100695.